Journal of Chromatography, 397 (1987) 47–70
Elsevier Science Publishers B.V., Amsterdam — Printed in The Netherlands

CHROMSYMP. 1148

HIGH-PERFORMANCE LIQUID CHROMATOGRAPHY OF AMINO ACIDS, PEPTIDES AND PROTEINS

LXXIII*. INVESTIGATIONS ON THE RELATIONSHIPS BETWEEN MOLECULAR STRUCTURE, RETENTION AND BAND-BROADENING PROPERTIES OF POLYPEPTIDES SEPARATED BY REVERSED-PHASE HIGH-PERFORMANCE LIQUID CHROMATOGRAPHY

MILTON T. W. HEARN* and M. I. AGUILAR
Department of Biochemistry, Monash University, Clayton, Victoria 3168 (Australia)

SUMMARY

The gradient retention behaviour in reversed-phase high-performance liquid chromatography of a series of polypeptides related to human β-endorphin has been investigated using different *n*-alkylsilica stationary phases and 0.1% trifluoroacetic acid in water–acetonitrile as mobile phase. In particular, the influence of changes in gradient time and flow-rate on retention parameters has been assessed with five different porous octadecylsilica phases with average particle diameters of 4 μm and 6 μm. Decreasing the pore size from 30 nm to 7.3 nm resulted in decreased S and log k'_0 values for most solutes. The effect of changes in the gradient steepness parameter, b, on the bandwidth behaviour of these polypeptides has also been investigated. Anomalous bandbroadening was observed for very steep and very shallow gradients, *i.e.* $b > 0.7$ or $b < 0.2$. The significance of these results is discussed in relation to the presence of hydrophobic domains in the linear sequence, the probability of the formation of highly stabilised secondary structures and the possible involvement of multiple folded forms of a single solute in the chromatographic performance of these polypeptides.

INTRODUCTION

The separation of polypeptides and proteins by reversed-phase high-performance liquid chromatography (RP-HPLC) has attracted much interest in recent years not only because of its enormous potential in biological applications but also for its power as a physico-chemical tool for the study of polypeptide/protein behaviour at hydrophobic liquid–liquid and liquid–solid interfaces including biological lipid bilayers. Arising from these investigations several fundamental approaches pertinent

* For Part LXXII see ref. 11.

0021-9673/87/$03.50

to the development of predictive optimisation models for the isocratic and gradient elution separation of peptides by RP-HPLC have been described[1–3]. In particular, relationships based on the linear solvent strength gradient model have been found [4–6] a useful tool for evaluating the retention behaviour of peptides and proteins separated under regular reversed-phase conditions. Utilising this approach, more optimal choice of flow-rate or gradient time conditions can be selected to enhance the resolution of a complex peptide mixture through improvement in bandspacing. For example, theoretical bandwidths, derived from theoretical quantitative plate height expressions, of some small peptidic molecules have been found to agree with the experimentally observed bandwidth values. However, in cases where stabilised secondary structural forms may be adopted by a peptide with half-lives comparable to the chromatographic residence times, experimental bandwidths significantly larger in magnitude than the theoretical bandwidths can arise. In order to clarify these phenomena further, the present paper provides a detailed analysis of the gradient elution data of a set of 29 polypeptides related to human β-endorphin on a range of octadecylsilica stationary phases with a trifluoroacetic acid–water–acetonitrile solvent system. In particular the retention and bandwidth behaviour under varying conditions of flow-rate and separation time has been interpreted in terms of the relationship between molecular structure, hydrophobic contact area and the predicted surface accessibility of the constituent amino acid residues.

MATERIALS AND METHODS

Apparatus

All chromatographic measurements were obtained using a Waters Assoc. (Milford, MA, U.S.A.) liquid chromatograph system consisting of two Model 6000A solvent delivery pumps, a U6K universal chromatographic injector, and an M660 gradient programmer. The detector used was an M450 variable-wavelength UV monitor operating at 215 nm and was coupled to a Hewlett-Packard 3390A plotter–integrator.

Chemicals and reagents

Acetonitrile was HPLC grade, obtained from Millipore (Lane Cove, Australia). Trifluoroacetic acid (TFA) was obtained from Pierce (Rockford, IL, U.S.A.). Water was quartz-distilled and deionised in a Milli-Q system (Millipore, Bedford, MA, U.S.A.). The human β-endorphin analogues were generously provided by Dr. Jan van Nispen (Organon, Oss, The Netherlands) and were repurified by semipreparative reversed-phase HPLC procedures immediately prior to use.

Chromatographic procedures

Bulk solvents and mobile phases were filtered and degassed under vacuum. Chromatographic measurements were made at 20°C using 25 cm × 4.6 mm I.D. stainless-steel columns packed with developmental dimethyloctadecylsilica of mean particle diameter of 6 μm, specific surface area of 380, 177, 143 and 45 m^2/g with corresponding average pore sizes of 7.3, 10.0, 13.0 and 30.0 nm, and alkyl chain coverages of 2.2, 2.2, 2.0 and 3.1 $\mu mol/m^2$, respectively as previously described[7]. The NovaPak C_{18} stationary phase, with a mean particle diameter of 4 μm and corre-

sponding average pore size of 9.0 nm and alkyl chain coverage of 3.0 μmol/m^2 was obtained as prepacked stainless-steel columns (15 cm × 3.9 mm I.D.) or radial compression cartridges (10 cm × 8 mm I.D.) from Waters Assoc., Linear gradient elution was carried out with 0.1% TFA in water (buffer A) and 0.1% TFA in water–acetonitrile (50:50) (buffer B) over gradient times varying between 20 and 120 min and flow-rates between 1 and 4 ml/min. All data points were derived from duplicate measurements, typically retention times varied by less than 0.5%. Sample sizes for each polypeptide were varied between 1 μg and 10 μg with injection volumes between 10 and 100 μl. No change in solute retention time for a defined gradient time was noted over this mass loading range. The column dead time, t_0, was taken as the retention time for sodium nitrate. The various chromatographic parameters b, S, $\bar{k}$, k_0, $\bar{\varphi}$, PC_{exp}, PC_{calc}, C, D_m, b', ρ, $\sigma_{v,calc}$ were calculated using the "Chained Pekinese" program written in BASIC language for a Hewlett-Packard HP86B computer using input values of t_0, F, t_g, t_G, $\Delta\varphi$, χ, γ, MW, d_p, a', $\sigma_{v,exp}$ and L as previously described[2,8].

RESULTS AND DISCUSSION

Retention relationships

It is generally accepted that the retention process for polypeptides and proteins in reversed-phase HPLC involves reversible binding of these polar solute molecules, P_1, P_2, P_3, . . . P_n, to accessible covalently bound ligands, L, at the surface of the stationary phase. Furthermore, previous studies have indicated that the adsorption process involves multisite interactions between hydrophobic regions on the polypeptide/protein surface and the chemically bonded non-polar ligand. This chromatographic process can thus be represented[9,10] in terms of a simplified non-mechanistic model such that

$$P(solv)_a + nL\ (solv)_b \underset{k_{-1}}{\overset{k_1}{\rightleftharpoons}} P(solv)_{(a-f)} \cdot nL + (nb + f)\ solv \qquad (1)$$

where n is the number of hydrocarbonaceous ligands associated with the protein at the stationary phase surface, a and b are the number of solvent molecules associated with the polypeptide/protein and each non-polar ligand respectively and f is the number of solvent molecules which occupy a surface area on the stationary phase equivalent to the interfacial hydrophobic contact area established between the polypeptide/protein and the non-polar surface.

In reversed-phase isocratic elution, the dependency of polypeptide or protein retention on the solvent mole fraction, φ, required to affect desorption has frequently been approximated to the linearised relationship

$$\log k' = \log k'_0 - S\varphi \qquad (2)$$

where k' is the capacity factor, k'_0 is the extrapolated k' at $\varphi = 0$ and S is the slope of the plot of $\log k'$ *versus* φ over a defined k' range. As the molecular weight (MW) of a peptide solute increases, the width of the operational solvent range $\Delta\varphi$ for regular reversed-phase retention behaviour is known from experimental studies to decrease significantly, such that over a practical k' range, *i.e.* $1 < k' < 20$, $\Delta\varphi$ values less than

0.05 may occur. One consequence of inappropriate $\Delta\varphi$ values is poor mass or bioactivity recovery. The dependency of S values on MW is now generally considered secondary[2,5] to the dependency of S values on the hydrophobic contact area of the solute, ΔA_h, occupied at the stationary phase surface.

Because of these pronounced dependencies of k' on φ, polypeptides and proteins are usually chromatographed on n-alkylsilicas under gradient elution conditions. The theoretical relationships between the gradient retention time t_g, the gradient steepness parameter b, the median capacity factor $\bar{k}$ and the corresponding organic mole fraction $\bar{\varphi}$ in linear and non-linear solvent strength gradients have been summarised in refs. 1, 2 and 4. Provided the retention of the polypeptide solute follows ideal linear solvent strength (LSS) gradient behaviour, $\bar{k}$ and $\bar{\varphi}$ are formally equivalent to the isocratic parameters k' and φ. Under regular reversed-phase gradient elution conditions, these parameters can therefore be related by analogy with eqn. 2 through the empirical expression

$$\log \bar{k} = \log \bar{k}'_0 - S\bar{\varphi} \tag{3}$$

The tangent S to the curve obtained in a plot of $\log \bar{k}$ *versus* $\bar{\varphi}$ can thus be determined at any particular value of $\bar{k}$ and the values of $\log \bar{k}$ at $\bar{\varphi} = 0$, or $\log k'_0$ can be obtained by extrapolation using regression analysis.

It has been previously noted[2–6,11,12] that several useful predictions arise from the above relationships if it is assumed that ideal reversed-phase behaviour of polypeptide solutes occurs under LSS gradient conditions. Under these conditions the gradient steepness parameter, b, is defined to be constant for all solutes. While both linear and non-linear dependencies of $\log \bar{k}$ on $\bar{\varphi}$ may be found experimentally, over the normally encountered range of $\Delta\varphi$, the relationship between $\log \bar{k}$ and $\bar{\varphi}$ has been evaluated in several studies (see *e.g.* refs. 2–6 and 9) in terms of linear dependencies. Differences in the reversed-phase gradient elution behaviour of a set of closely related peptide solutes of well-defined primary structure should directly relate to the influence of the amino acid side chains, and "on-column" structural differences which in principle can be correlated with functional group parameters. More specifically, changes in the b value will lead to selectivity changes for peptides with different S values, *i.e.* where the mechanism of interaction with the stationary phase involves different equilibrium and kinetic rate constants. This non-parallelism in the $\log \bar{k}$ *versus* $\bar{\varphi}$ plots presumably arises through the participation of different classes of binding sites on the heterogeneous stationary phase surface, through the involvement of different topographic regions on the solute surface, or through a combination of both processes. Determination of the S and $\log k'_0$ values therefore represents the first step in investigating the mechanistic details of the interaction between the stationary phase and the peptidic solute.

For a given peptide separated on two different columns of identical dimensions, but containing alkylsilicas of pore diameters m and n respectively, and eluted with the same mobile phase, the relationship between relative retention, k, and non-polar surface area, A_L, in the columns is given[7] by

$$\frac{k_m}{k_n} = \frac{K_{RP,m}}{K_{RP,n}} \cdot \frac{d_{L,m}}{d_{L,n}} \cdot \frac{A_{L,m}}{A_{L,n}} \cdot \frac{V_{sec,n}}{V_{sec,m}} \tag{4}$$

where K_{RP} is the reversed-phase retention distribution coefficient, d_L is the effective thickness of the hydrocarbonaceous ligand for a maximally bonded silica-based packing material and V_{sec} is the retention volume of the solute that is not due to interaction with the hydrophobic surface. At a fixed organic solvent content φ, both the K_{RP} and d_L terms will be constant, provided the solvent extraction and solute adsorption isotherms for the two different stationary phases are equivalent. In these cases a linear relationship between relative retention and ligand surface area will exist, that is

$$\frac{k_m}{k_n} = \frac{A_{L,m}}{A_{L,n}} \cdot \frac{V_{sec,n}}{V_{sec,m}} \tag{5}$$

If only a fraction of the non-polar surface area within the pores of the second stationary phase can be accessed by the peptide due to various solute–ligand conformational constraints eqn. 5 reduces to

$$\frac{k_m}{k_n} = \frac{f_m A_{L,m}}{f_n A_{L,n}} \cdot \frac{V_{sec,n}}{V_{sec,m}} \tag{6}$$

where f_i is the fractional accessibility factor and is dependent on the composition of both the solute and mobile phase. The magnitude of the f_i-factor will therefore influence the reversed-phase component of retention, while the molecular volume of the solute will affect the size exclusion component.

When solutes are excluded from the stationary phase pores, the value of the f_i-factor will be related to the bonded surface area outside the pores. The total non-polar surface area, A_L is the sum of the bonded surface area inside, A_p, and outside, A_0, that is,

$$A_L = A_p + A_0 \tag{7}$$

While A_p is $\gg A_0$ for most stationary phases, the retention of a totally excluded polypeptide or protein may still be significant with non-porous *n*-alkylsilica media if the reversed-phase distribution coefficient, K_{RP} is very large[13,14]. A number of factors may give rise to restricted movement of solutes into the pores. Firstly, the binding of a solute molecule at the entrance of a pore chamber will decrease the effective pore accessibility to a second solute molecule. A second effect arises from restricted diffusion associated with the hydrodynamic drag on the diffusing solute due to the proximity of the pore walls, and thirdly, many polypeptides or proteins show a tendency to undergo aggregation either in solution or at solid–liquid interfaces. All of these effects will limit solute permeability into/from the pores.

Dependence of polypeptide capacity factor on organic solvent mole fraction

In order to further investigate the intimate relationship between peptide structure and chromatographic behaviour in reversed-phase systems, the present work was initiated to extend our previous studies on the retention characteristics of various polypeptide hormone analogues. In particular, the current investigation was addressed to a detailed analysis of the structure–retention relationships of 29 synthetic

TABLE I

STRUCTURES AND RETENTION PARAMETERS OF HUMAN β-ENDORPHIN-RELATED POLYPEPTIDES CHROMATOGRAPHED ON DIFFERENT ALKYLSILICA STATIONARY PHASES

The S and log k'_0 values were determined by linear regression analysis according to eqn. 8. Columns: 6 μm dimethyloctadecylsilicas of 7.3 nm (1), 10 nm (2), 15 nm (3) and 30 nm (4) average pore diameter were packed into 25 cm × 4.6 mm I.D. stainless-steel columns: 4 μm Novapak dimethyloctadecylsilicas were packed into radial compression cartridges (10 cm × 8 mm I.D.) (5) or stainless-steel columns (15 cm × 3.9 mm I.D.) (6).

Peptide	*Sequence*	*MW*	*S*						*log k'₀*					
			1	*2*	*3*	*4*	*5*	*6*	*1*	*2*	*3*	*4*	*5*	*6*
1	YGGFM	573	7.7	8.6	10.0	10.8	12.4	13.7	2.5	2.6	2.8	2.4	3.3	3.2
2	YGGFMTS	761	9.4	10.5	11.2	12.9	14.8	17.8	2.6	2.7	2.9	2.5	3.4	3.6
3	YGGFMTSEKSQTPLVT	1744	11.6	13.0	14.2	16.7	23.4	27.0	3.4	3.8	4.2	3.8	5.4	6.2
4	YGGFMTSEKSQTPLVTL	1859	11.3	12.6	13.1	14.8	21.1	25.2	4.0	4.2	4.7	4.2	6.0	6.8
5	YGGFMTSEKSQTPLVTLFK	2134	11.5	11.5	13.1	14.3	25.8	28.4	4.4	4.5	5.3	4.6	7.5	8.1
6	YGGFMTSEKSQTPLVTLFKNAIIKNAYKKGE	3263	15.2	9.3	15.1	15.2	56.6	45.9	6.1	4.8	6.9	5.7	15.4	13.0

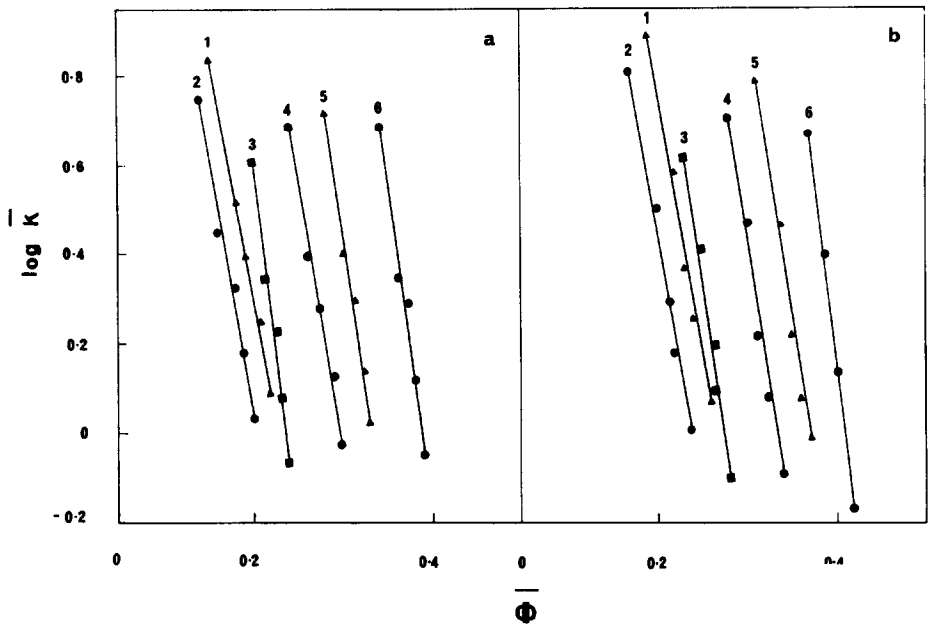

Fig. 1. Plot of log $\bar{k}$ *versus* $\bar{\varphi}$ for the human β-endorphin-related polypeptides 1–6 (Table I). The plots were derived from best-fit analysis to the data obtained, where t_G = 20, 30, 40, 60 and 120 min and the flow-rate (F) 1 ml/min (data points included), and F = 1, 2, 3 and 4 ml/min and t_G = 40 min (data not shown). Experiments were carried out with 6 μm octadecylsilica with an average pore diameter of 7.3 nm (panel a) or 10.0 nm (panel b), packed into a 25 cm × 4.6 mm I.D. stainless-steel column. Other chromatographic conditions are given in Materials and methods. See Table I for the peptide structures and derived S and log k'_0 values.

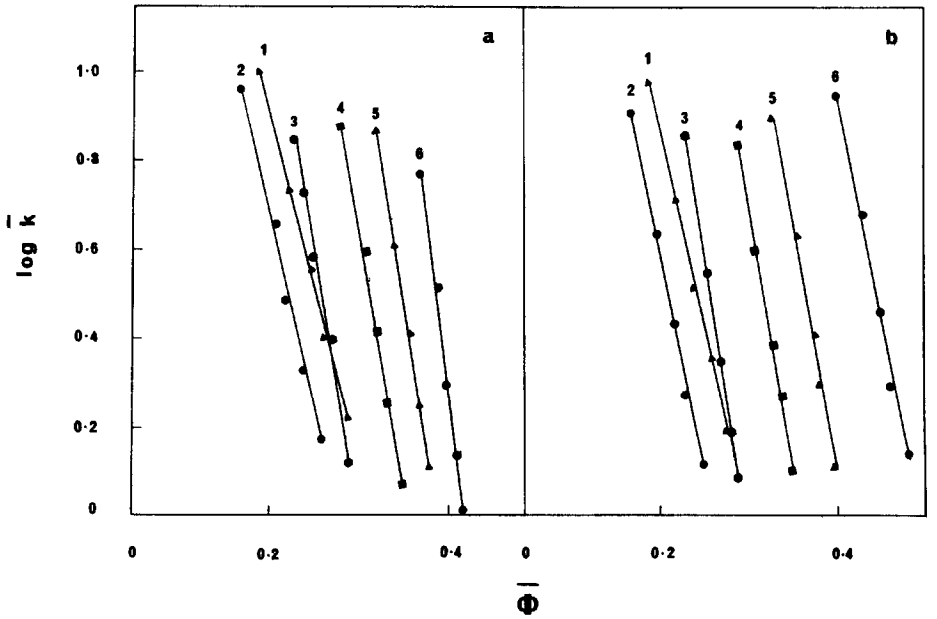

Fig. 2. Plot of log $\bar{k}$ *versus* $\bar{\varphi}$ as in Fig. 1. Details and conditions as in Fig. 1 except octadecylsilica with an average pore diameter of 13.0 nm (panel a) and 30.0 nm (panel b).

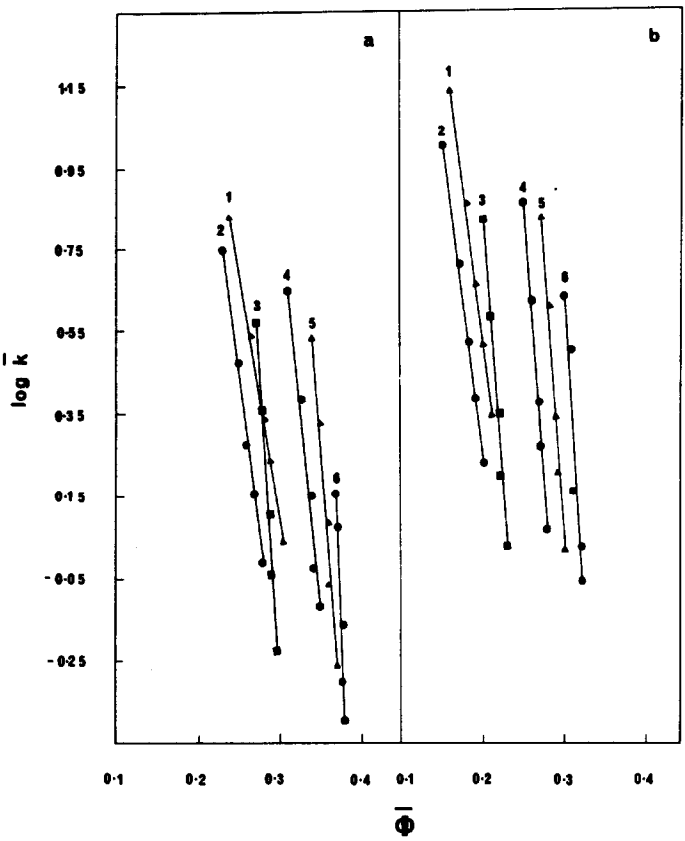

Fig. 3. Plot of log $\bar{k}$ *versus* $\bar{\varphi}$ as in Fig. 1. Details and conditions as in Fig. 1 except NovaPak octadecylsilica packed into radial compression cartridges (10 cm × 8 mm I.D.) (panel a) and stainless steel columns (15 cm × 3.9 mm I.D.) (panel b).

peptide analogues related to human β-endorphin and includes new data pertinent to the underlying structural origin of differences in bandwidth behaviour seen for α-endorphin, γ-endorphin and β-endorphin. The structures of these latter peptides are listed in Table I (peptides 1–6), and represent amino-terminal analogues ranging between 5 and 31 amino-acid residues in size. Gradient elution data were collected on various octadecylsilica supports, the characteristics of which are given in Materials and methods section.

As part of one series of experiments, values of $\bar{k}$ and $\bar{\varphi}$ were calculated from the gradient retention times (t_g) of these six peptides for gradient times of t_G = 20, 30, 40, 60 and 120 min at a flow-rate of 1 ml/min. In a second series of experiments, the gradient time was held constant at 40 min, while separations were carried out at flow-rates of 1, 2, 3 and 4 ml/min for each of the six columns. All samples were chromatographed in triplicate using a linear gradient from 0.1% TFA in water to 0.1% TFA in acetonitrile–water (50:50, v/v). Figs. 1–3 show the plots of log $\bar{k}$ *versus* $\bar{\varphi}$ for the six endorphin analogues. As is evident from the experimental data essentially linear dependencies were observed over the retention range $1 < \bar{k} < 10$. The cor-

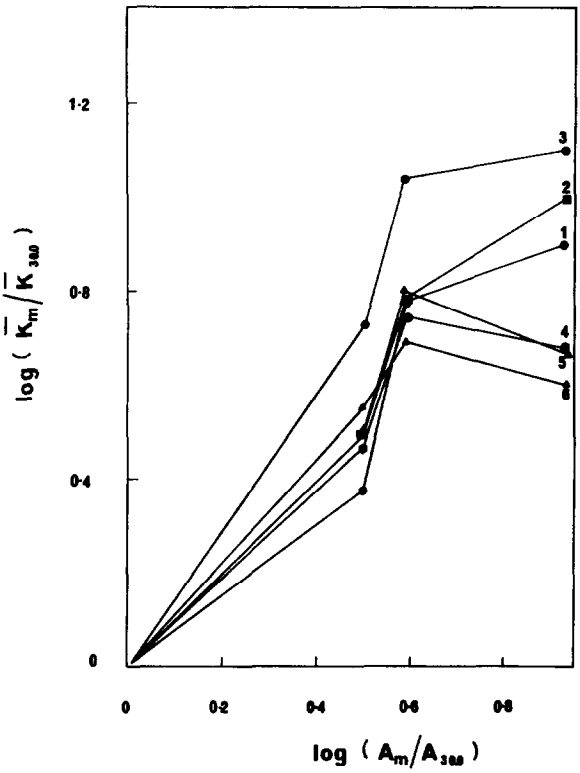

Fig. 4. Plots of relative retention *versus* hydrocarbonaceous surface area of the developmental octadecylsilica stationary phases. The data shown were derived for $\bar{\varphi} = 0.3$ and other conditions as given in the legend for Fig. 1.

relation coefficients for the linear regression analysis of the log $\bar{k}$ *versus* $\bar{\varphi}$ data were between 0.90 and 1.00 for all six peptides on all columns with the exception of peptide 6 on the NovaPak supports where r^2 was equal to 0.79.

If all the hydrophobic surface area of the stationary phase was accessible to the solute, retention would be expected to be proportional not only to the solutes hydrophobic contact area but also to the number of μmoles of non-polar ligand per unit volume within the column. Fig. 4 shows the plots of relative retention of these six endorphin analogues (at $\bar{\varphi} = 0.3$) *versus* the corresponding surface area ratio ($A_{L,m}/A_{L,30}$) of four developmental *n*-alkylsilica columns, *i.e.* relative to the 30 nm pore diameter stationary phase. It can be seen that the retention behaviour of peptides 1–3 shows small increases in $\bar{k}$ with increasing stationary phase surface area per ml column bed. Similarly, the apparent retentivities of the higher molecular weight solutes also increase with increasing stationary phase surface area, *i.e.* from the 30 nm to the 10 nm pore diameter stationary phase, but show apparent retention decreases with the 7.3 nm against pore diameter support. When $\bar{k}$ values at $\bar{\varphi} = 0.3$ are plotted against μmoles alkyl chain per gram of stationary phase for the various supports (Fig. 5), the plots illustrate a more normalised relationship to that observed between relative retention and stationary phase surface area. It therefore appears from these

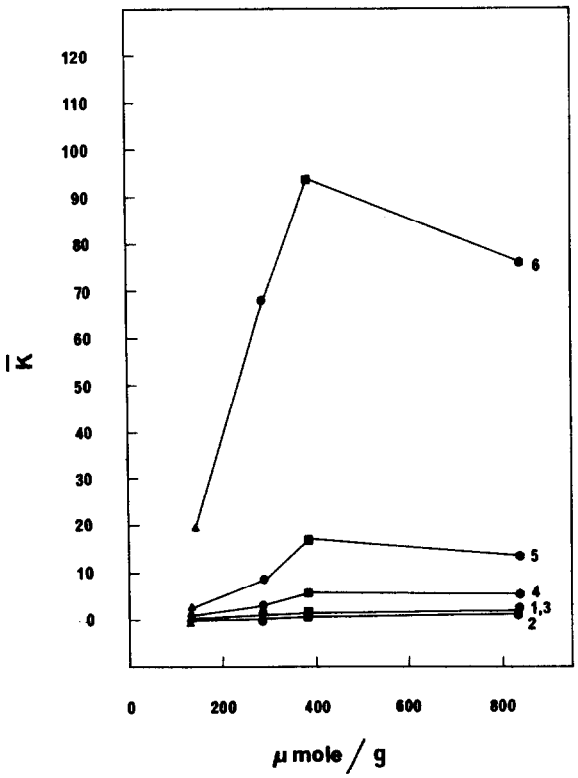

Fig. 5. Plots of median capacity factor *versus* ligand density (in μmole alkyl chain per gram packing material) for the four developmental octadecylsilica packings. The data were derived for $\bar{\varphi} = 0.3$, and other conditions as given in the legend for Fig. 1.

data that not all the hydrophobic bonded surface area of the 7.3 nm pore diameter support material is accessible tot peptides 4–6 which thus exhibit retention properties similar to those observed with stationary phases of lower alkyl chain coverage.

Previous studies[7,12] on the reversed-phase chromatography of phenylalanine oligomers using columns packed with these same four dimethyloctadecylsilica supports have shown similar results. In these earlier studies it was demonstrated that the relative retention of solutes of MW $\leqslant$ 500 at a fixed mobile phase composition decreased as the pore size of the particle increased. However, for intermediate solutes (MW 1000–3000) the retention increased from the 30 nm to the 10 nm pore diameter support but then decreased with the 7.3 nm pore diameter support. In contrast, the apparent retention as a function of log $(A_{L,m}/A_{L,30})$ of larger proteins (MW 10^4–$7 \cdot 10^4$) decreased monotonously as the pore size decreased. As all these comparative studies were carried out with mobile phases of similar isocratic composition, it was concluded that the decrease in apparent k' observed at larger log $(A_{L,m}/A_{L,30})$ values with this (limited) group of biosolutes reflected the progressive restriction of these solutes from the pore chambers due to a combination of molecular volume increases for the solutes corresponding to MWs over the range $2 \cdot 10^2$–$7 \cdot 10^4$ and decreases in the average pore diameter of the particles with common diameter (*ca.* 6 μm) over

the range 30 nm to 7.3 nm. The logical endpoint of such decreases in average pore diameter would be a non-porous particle of equivalent particle diameter. Based on the above relative retention trends, smaller S and log k' values would be predicted for such non-porous *n*-alkylsilica supports. Recent studies[13,14] from this laboratory with such non-porous *n*-alkylsilica stationary phases are consistent with this behaviour for both small peptides and large globular proteins.

Differences in the selectivity for the human β-endorphin peptides when chromatographed on each of the different column types are clearly reflected in the different slopes or S values which are listed in Table I. As has been previously discussed[5] in detail elsewhere, polypeptide or protein S-values can be related directly to the hydrophobic contact area established by the solute at the stationary phase surface. In conjunction with the results shown in Fig. 5, it appears that despite the increasing carbon content of the different stationary phases, the decrease in pore size lowers the accessible interactive surface area for interaction between the stationary phase and the solute. Indeed, it has been found that S values for a range of peptides and proteins chromatographed on non-porous reversed-phase silica supports are significantly lower than on an equivalent porous support. In other words, the retention properties of the current series of peptide analogues on the 7.3 nm pore diameter packing material are more characteristic of polypeptide separations carried out on non-porous *n*-alkylsilica stationary phases[13,14]. In this context, it is thus of interest that much higher values of S and log k'_0 were obtained using the NovaPak stationary phase (4 μm mean particle diameter with nominal surface area 9.0 nm pores) than the 6-μm octadecylsilica phase of nominal 10 nm pore diameter. In addition, the difference between these S and log k'_0 values for the NovaPak and developmental packings for each solute increased as the molecular weight of the peptide increased. For example, while the S values for peptide 1 were similar on both packing types, the corresponding NovaPak values for peptide 6 were higher by a factor of between three and four. Although the pore size and percent carbon loading of the NovaPak columns are similar to the 10-nm pore diameter developmental packing, the differences in particle diameter, the base silica matrix and the manufacturing process have clearly produced a stationary phase of significantly different interactive properties.

Studies on the bandwidth behaviour of the human β-endorphin peptides (1–6) with the various hydrophobic stationary phases used in this investigation have been previously documented[8]. The results illustrated significant divergences between the experimentally observed peak widths from theoretical peak widths predicted from the general plate height theory. In particular, the degree of disparity between the experimental ($\sigma_{v,exp}$) and the calculated ($\sigma_{v,calc}$) bandwidth values for β-endorphin varied significantly with the different columns, despite the close similarity in the packing types. It is apparent therefore, that the mechanistic processes involved in the passage of peptidic solutes through the porous support and the associated adsorption–desorption phenomena are more complex than may be anticipated on the basis of simple diffusional properties of smaller solute molecules. The involvement of complex conformational equilibria and its effect on the thermodynamic and kinetic processes of solute zone migration is now receiving serious experimental and theoretical consideration in this and other laboratories. As part of these studies, the bandwidth relationships of a larger series of β-endorphin-related analogues were investigated in relation to the possibility that highly stabilised secondary–tertiary struc-

TABLE II

CHARACTERISTICS OF THE POLYPEPTIDES RELATED TO HUMAN β-ENDORPHIN USED IN THE STUDY OF BANDWIDTH BEHAVIOUR

Peptide	*Sequence*	*Position in β-endorphin*	*Number of residues*	*MW*	*S**	log k'_0	$D_m \cdot 10^7$ (cm^2/s)
1	YGGFM	1–5	5	573	10.0	2.8	3.4
2	YGGFMTS	1–7	7	761	11.2	2.9	3.1
3	YGGFMTSEKSQTPLVT	1–16	16	1744	14.2	4.2	2.4
4	YGGFMTSEKSQTPLVTL	1–17	17	1859	13.1	4.7	2.3
5	YGGFMTSEKSQTPLVTLFK	1–19	19	2134	13.1	5.3	2.2
6	YGGFMTSEKSQTPLVTLFKNAIIKNAYKKGE	1–31	31	3263	15.1	6.9	1.9
7	GGFM	2–5	4	410	9.0	2.3	3.8
8	GGFMT	2–6	5	511	9.7	2.2	3.5
9	GGFMTS	2–7	6	598	14.6	2.5	3.4
10	GGFMTSE	2–8	7	727	11.6	2.6	3.1
11	GGFMTSEK	2–9	8	855	10.9	2.3	3.0
12	GGFMTSEKSQ	2–11	10	1070	13.3	2.6	2.8
13	GGFMTSEKSQTP	2–13	12	1268	14.3	3.1	2.6
14	GGFMTSEKSQTPLVT	2–16	15	1581	15.2	4.1	2.4
15	GGFMTSEKSQTPLVTL	2–17	16	1694	13.7	4.5	2.4
16	GGFMTSEKSQTPLVTLF	2–18	17	1841	12.8	5.1	2.3
17	GGFMTSEKSQTPLVTLFK	2–19	18	1969	14.0	5.3	2.3
18	TSEK	6–9	4	473	**	**	3.6
19	MTSEK	5–9	5	594	20.0	1.3	3.4
20	FMTSEK	4–9	6	741	13.3	2.9	3.1
21	IIKNAYKKGE	22–31	10	1162	15.8	2.5	2.7
22	FKNAIIKNAYKKGE	18–31	14	1622	15.8	3.6	2.4
23	LVTL	14–17	4	444	10.8	2.6	3.7
24	SQTPLVTL	10–17	8	857	13.7	3.5	3.0
25	KSQTPLVTL	9–17	9	985	13.1	3.4	2.8
26	EKSQTPLVTL	8–17	10	1114	13.4	3.6	2.7
27	SEKSQTPLVTL	7–17	11	1201	13.9	3.6	2.7
28	TSEKSQTPLVTL	6–17	12	1302	14.0	3.5	2.6
29	MTSEKSQTPLVTL	5–17	13	1433	14.2	3.7	2.5

* Average values determined from regression analysis according to eqn. 8.

** The S and log k'_0 values of peptide 18 are not included due to the very short retention time of this peptide.

tures occur with these peptides during reversed-phase chromatographic separation process.

Bandwidth relationships

Under gradient elution conditions, the peak capacity, PC, for a chromatographic separation of gradient time, t_G, and average resolution equal to unity for all adjacent peaks is given by

$$PC = t_G/4\sigma_t \quad (8)$$

where σ_t is the bandwidth measured in time units (one standard deviation). The equations which describe the theoretical relationship between σ_v and $\bar{k}$ for LSS systems have been previously summarised[1,8]. In earlier studies on the reversed-phase gradient elution of synthetic analogues of β-endorphin[2,8] luteinizing hormone releasing hormone[5], gonadotropin hormone releasing factor[5] and myosin light chain kinase[11] we demonstrated that gradient retention behaviour for a number of these polypeptide solutes can be closely predicted using the equations derived from LSS theory. In some cases the experimental bandwidth also closely approximated the bandwidth calculated according to the general plate height theory derived for the separation of small low-molecular-weight solutes. However, in other cases, there were significant divergencies between the experimental and "ideal" bandwidths at longer column residence times, where changes in peptide secondary–tertiary structure could, in principle, occur.

The present study extends the previous retention and bandwidth investigations by providing further data on the bandwidth behaviour of the series of 29 peptides related to human β-endorphin on an octadecylsilica support with a nominal pore diameter of 13 nm. The structures of these peptides are listed in Table II. The peptides can be generally divided into five main groups encompassing the amino-terminal, carboxy-terminal and internal endo regions of human β-endorphin. These peptides range in size from 4 to 31 residues with a molecular weight range of *ca.* 400–3500. This series of closely related peptides thus provides an excellent opportunity to directly relate differences in retention and bandwidth properties to the primary and higher hierarchical structures of these solutes.

It is well established that in gradient elution chromatography, the median capacity factor $\bar{k}$, and the experimental peak width $4\sigma_t$, of low-molecular-weight organic solutes are inversely proportional to the gradient steepness parameter, b. Such inverse dependencies between $\bar{k}$ and b have also been observed for polypeptides and proteins separated under reversed-phase and hydrophobic interaction chromatographic modes (see for example refs. 2–6, 8 and 9). In a number of cases, the experimental bandwidths of polypeptide solutes have also followed the same theoretical dependence on b as is observed for low-molecular-weight solutes. In such cases the kinetics of secondary retention phenomena are assumed to be either very fast or very slow when compared to the average mass transport process. There are, however, an increasing number of examples where the average relaxation times associated with conformational, orientational, aggregative or other solute-dependent secondary equilibrium processes are of comparable magnitude to the mass transfer time[9,15,16].

In general, a peptide or protein may interact with the stationary phase through

the participation of a number of different topographic sites or domains or through the participation of several aggregative forms etc., all of which may be present in either native conformation or in various unfolded states. As a consequence the apparent retention and band-broadening for a particular polypeptide must reflect its time-averaged behaviour as it passages down the chromatographic bed. It is worth restating here our tenet that biopolymer HPLC, irrespective of whether it involves interactive or non-interactive support media, should be viewed in an analogous way to a chemical reactor bed in which time-dependent processes other than simple longitudinal or transverse mass transport occurs under the influence of the flowing mobile phase. When viewed in this way, conformational and reorientational behaviour of a peptide solute during chromatographic experiments represents a set of topographic structural "intermediates" which may or may not result in the elution of a single time-averaged species with retention and band-broadening characteristics in accord with those predicted solely on the basis of primary sequence or molecular size as derived from the amino acid composition or the molecular weight. Most current theoretical approaches which describe the thermodynamic and kinetic processes of macromolecular solute migration in interactive HPLC systems do not yet quantitatively address the implications of a single solute with multiple interaction sites or varying diffusional properties and molecular shape as a consequence of time-dependent exposure to a particular chromatographic environment. For example the derivation of the theoretical equation for σ_v, namely

$$\sigma_v = [t_G F (1 + 1/\bar{k})] / (\ln 10) N^{0.5} S \Delta\varphi = [(\bar{k}/2) + 1] G t_0 F N^{-0.5} \quad (9)$$

is based on the assumption that the shape of a peptidic solute of defined molecular weight can be characterised in terms of a constant hydrodynamic shape throughout the chromatographic separation. Under these conditions, it would be anticipated that the normalised ratio of the experimentally observed bandwidths to the calculated bandwidths ($\sigma_{v,exp}/\sigma_{v,calc}$) should approach unity over the normal operational range of $\bar{k}$ values. If, however, during a chromatographic experiment, multiple unfolded forms of a polypeptide or protein solute are generated, each of which has significantly different retention and/or diffusional properties, the experimentally observed peak width will be significantly different to that predicted by equations based on the general plate height theory. Figs. 6–9 compare the experimentally observed peak widths to the theoretical peak width values for the range of 29 β-endorphin-related peptides. The ratio of experimental to calculated bandwidth, $\sigma_{v,exp}/\sigma_{v,calc}$ is plotted as a function of the inverse of the gradient steepness parameter, $1/b$. Panel a in each figure represents the data accumulated for a constant flow-rate and varied gradient time t_G, while the data in panel b were obtained at a constant t_G and varied flow-rate. In Figs. 6a–9a, there is a parabolic dependence of the bandwidth ratio on $1/b$ with the minima between $b = 0.3$–0.5. The large discrepancies between the two bandwidth values at high b-values or steep gradients are probably related to the fact that stepwise elution rather than linear gradient conditions are experienced by the solute under these conditions. If it is argued that with very steep gradients the solvent percentage of the mobile phase surpasses the optimal φ-value that is required to reach the minimum in the log k' *versus* σ plot[17] then the increases in band-broadening observed for polypeptides under these conditions may reflect the increasing contribution of sil-

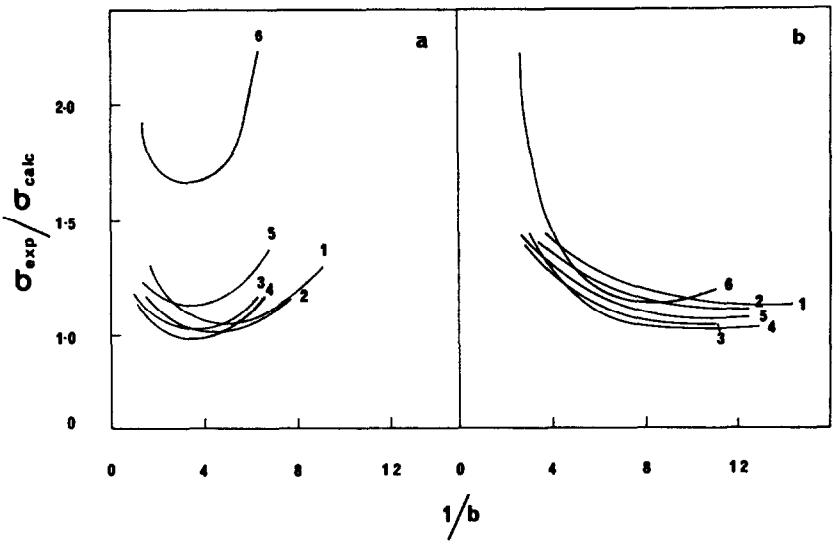

Fig. 6. Plots of $\sigma_{v,exp}/\sigma_{v,calc}$ *versus* $1/b$ for β-endorphin-related peptides 1–6 (Table II). Data acquired under conditions of different gradient time, t_G = 20, 30, 40, 60 and 120 min and F = 1 ml/min (panel a) and varied flow-rate, F = 1, 2, 3 and 4 ml/min and t_G = 40 min (panel b) (Experimental data points omitted for clarity). Experiments carried out were with 6 μm octadecylsilica with an average pore diameter of 13 nm, packed into a 25 cm × 4.6 mm I.D. stainless-steel column. The value of $\sigma_{v,calc}$ is calculated from eqn. 9, *i.e.* $\sigma_{v,calc} = t_0 FN^{-0.5} (k/2 + 1) G$ and $\sigma_{v,exp}$ was determined for each solute by direct measurement. Other conditions are given in Materials and methods.

anophilic interactions to the overall chromatographic behaviour. As a consequence, normal band-sharpening due to increases in solvent strength as estimated by the G value do not occur, and the experimentally observed bandwidth is larger than the calculated value. Although the deviation of the bandwidth ratio (σ_{exp}: σ_{calc}) from unity at low b-values or long gradient times has yet to be adequately explained, this effect must also be related to solute-specific physico-chemical phenomena associated

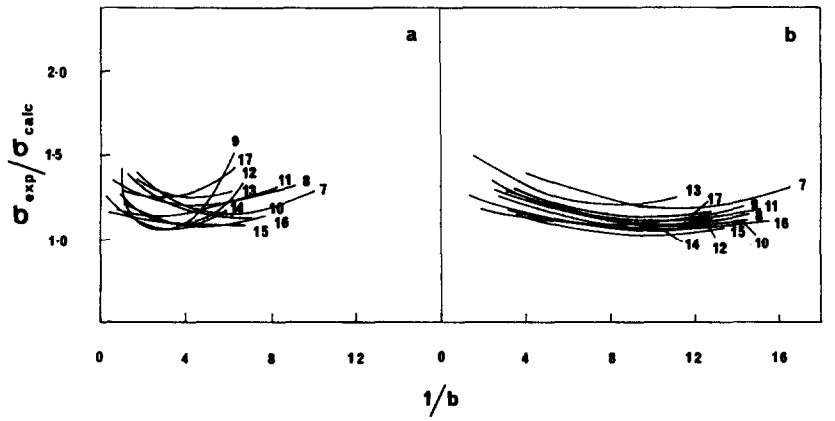

Fig. 7. Plots of $\sigma_{v,exp}/\sigma_{v,calc}$ *versus* $1/b$ for peptides 7–17 (Table II). Other details and conditions as given in the legend for Fig. 6.

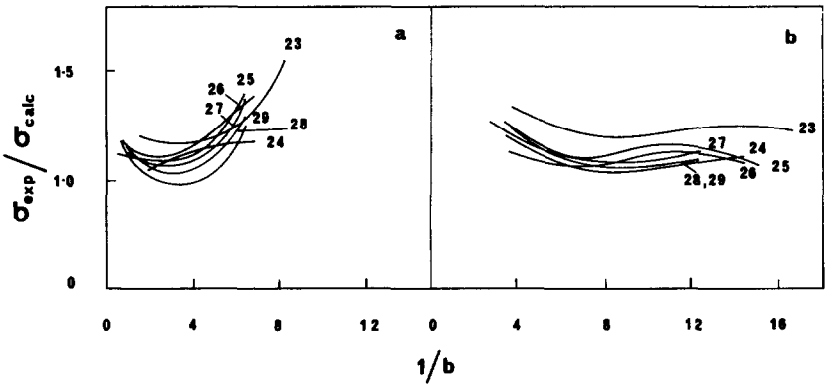

Fig. 8. Plots of $\sigma_{v,exp}/\sigma_{v,calc}$ *versus* $1/b$ for peptides 19–22 (Table II). Other details and conditions as given in the legend for Fig. 6.

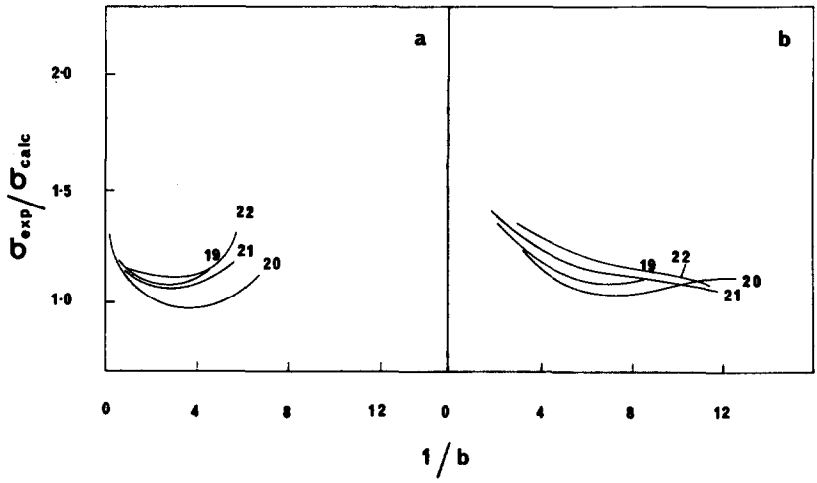

Fig. 9. Plots of $\sigma_{v,exp}/\sigma_{v,calc}$ *versus* $1/b$ for peptides 23–29 (Table II). Other details and conditions as given in the legend for Fig. 6.

with solute–stationary phase interactions. Clearly, conformational reorientation of peptides at non-polar surfaces may explain this anomalous behaviour of, for example β-endorphin (peptide 6). Figs. 6b–9b illustrate a further facet of the effect of column residence time on the experimental bandwidth, where the σ_v ratio steadily decreases asymptotically from a maximum at the slowest mobile phase flow-rate of 1 ml/min.

Further interpretation of these bandwidth data can be made through the comparison of the experimental peak capacity data with the calculated peak capacity data. It has been previously demonstrated[8] that experimental retention data can be used to calculate a predicted peak capacity according to the relationship

$$PC = \left(\frac{\ln 10}{4}\right)\left(\frac{S\Delta\varphi\,\bar{k}^{0.25}}{Fd_p}\right)\left(\frac{D_m\,t_0}{C}\right)^{0.5} \qquad (10)$$

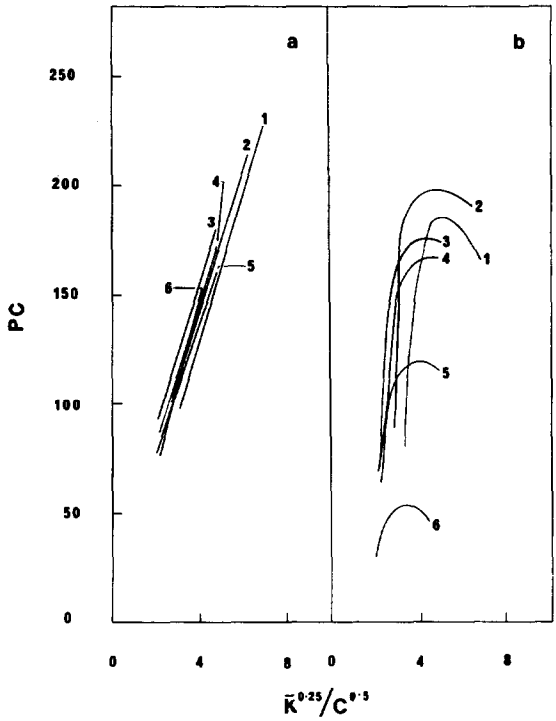

Fig. 10. Plots of peak capacity (PC) *versus* $\bar{k}^{0.25}/C^{0.5}$ for the β-endorphin-related peptides 1–6 (Table II). The data correspond to calculated values obtained for the varied t_G experiments (t_G = 20, 30, 40, 60 and 120 min) and F = 1 ml/min. (a) PC value determined from eqn. 10. (b) PC value calculated from eqn. 8. Experiments were carried out with 6 μm octadecylsilica with an average pore diameter of 13 nm packed into a 25 cm × 4.6 mm I.D. stainless-steel column. Experimental data points are omitted for clarity. Other details and conditions are given in Materials and methods.

For peptides separated under defined gradient elution conditions, where a regular reversed-phase mechanism is operating, linear dependencies would thus be anticipated between the peak capacity PC and $\bar{k}^{0.25}/C^{0.5}$. Figs 10–13 show the plots of PC *versus* $\bar{k}^{0.25}/C^{0.5}$ for the 29 β-endorphin analogues at a constant flow-rate of 1 ml/min and varied t_G. Panel a in each diagram is the predicted peak capacity calculated according to eqn. 10 and panel b in each case represents the experimental PC estimated from eqn. 8. In Fig. 10, the experimental peak capacity of peptides 1–5 closely approximated the predicted values except at very low b values, where the dependencies reached a maximum. A similar dependency was observed for β-endorphin (peptide 6), but the experimental peak capacity was significantly lower than would be expected for a peptide of the same MW and $\bar{k}$ values. Fig. 11 shows the PC plots for the endo series of analogues where close agreement between the experimental and predicted peak capacities is observed. In Fig. 12, essentially linear dependencies between PC_{exp} and $\bar{k}^{0.25}/C^{0.5}$ were observed for peptides 19–22 but in all cases the magnitude of PC_{exp} was lower than PC_{calc}. In Fig. 13 the data for the internal spacer series of analogues is presented. The experimentally observed peak capacity of all peptides except peptide 24 exhibits an asymptotic dependency on $\bar{k}^{0.25}/C^{0.5}$ with the

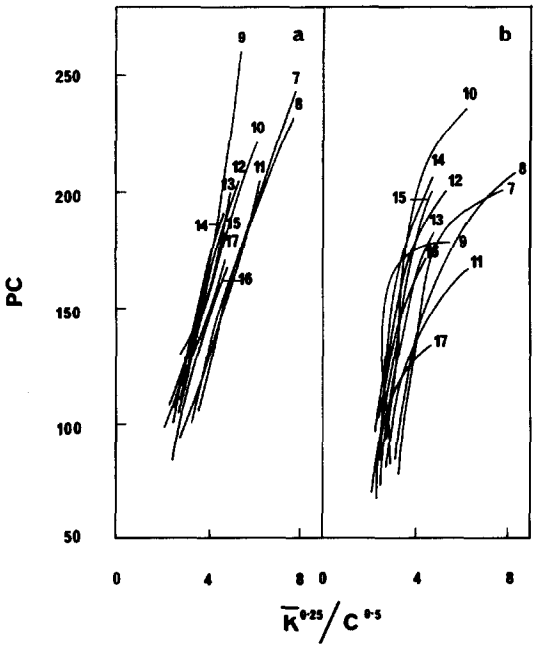

Fig. 11. Plots of PC *versus* $\bar{k}^{0.25}/C^{0.5}$ for β-endorphin-related peptides 7–17 (Table II). Other experimental conditions are described in the legend for Fig. 10.

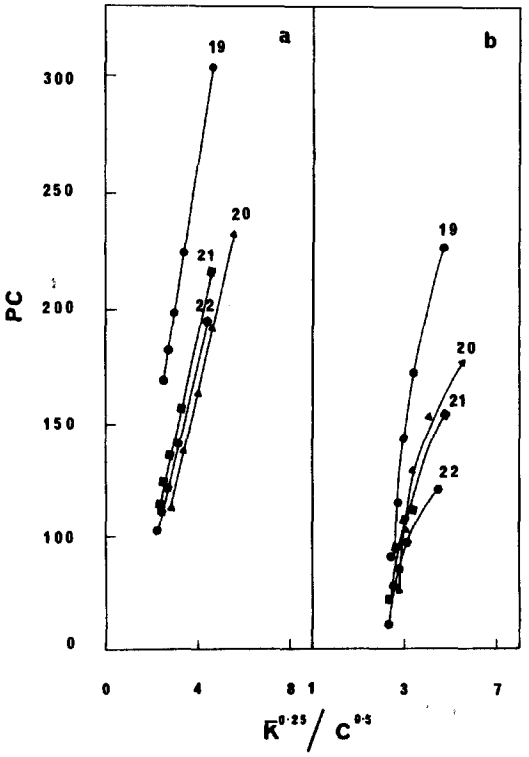

Fig. 12. Plots of PC *versus* $\bar{k}^{0.25}/C^{0.5}$ for β-endorphin-related peptides 19–22 (Table II). Other experimental conditions are described in the legend for Fig. 10.

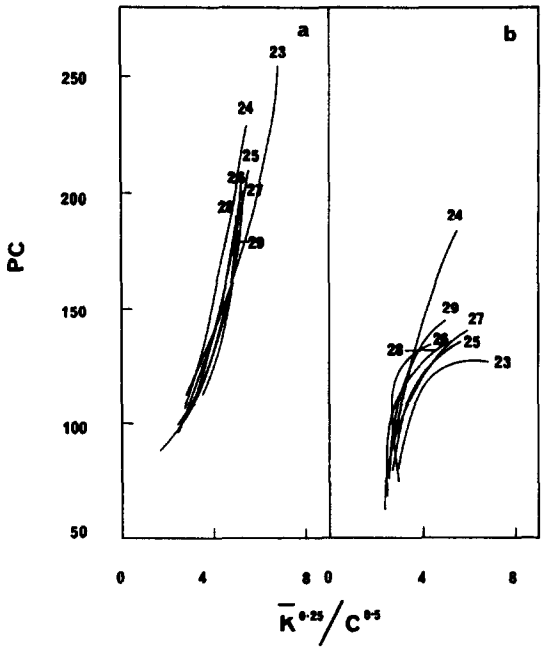

Fig. 13. Plots of PC *versus* $\bar{k}^{0.25}/C^{0.5}$ for β-endorphin-related peptides 23–29 (Table II). Other experimental conditions are described in the legend for Fig. 10.

value of PC_{exp} decreasing rapidly with decreasing *b*. Thus, with the four families of related peptides studied in this investigation, there is a remarkable range of bandwidth behaviour. The relationship used to calculate PC_{calc} assumes that a peptide will behave as a conformationally invariant species during the passage along the reversed-phase support. If indeed this occurs, incorporation of the diffusion coefficient D_m in eqn. 9 essentially normalises the data for the effects of molecular weight and size on the kinetic properties of the peptidic solute. The explanation for the differences in the peak capacity behaviour for these β-endorphin related analogues must reside, as previously noted, in the nature of the intimate association between solute solvation and solute conformation in the extraparticulate and intraparticulate spaces at the stationary phase surface. The influence of such effects, including the heterogeneity of the pore structure on polypeptide band-broadening, has yet to be quantitatively determined. Indeed, quantitative discussion of all aspects of the influence of polymodal porous structure *per se* on the thermodynamic and kinetic properties of peptide migration has only recently been feasible due to the development of improved analytical tools including the development of non-porous stationary phases with particle diameters between 0.75 and 2.1 μm. However, while anomalous bandwidth behaviour may be in part due to the complex kinetics associated with the migration of biopolymer solutes through the polydisperse porous structure of reversed-phase packings, it is the molecular composition of the interactive segment of the solute which presents itself to the chromatographic surface that ultimately determines the thermodynamic properties of the solute. Furthermore, it is the number of interactive species derived from a single solute, and the corresponding range of

thermodynamic and kinetic properties of those species, which will be responsible for the experimentally observed bandwidth behaviour.

The estimation of which part of a polypeptide is involved in the binding to the stationary phase under a defined set of conditional parameters would therefore give some insight and predictive power into the chromatographic behaviour of a particular polypeptide. In this regard, a battery of peptide secondary and tertiary structure determinations is required. However, in the first instance, considerable information can be obtained from the determination of hydropathy profiles based on the amino acid sequence of a peptide. This approach involves the summation of individual hydrophilicity parameters for each residue of a seven-residue segment of a polypeptide or protein, and assigning this value to the fourth residue. The reading frame is then transposed by one residue at a time along the chain. Fig. 14 shows the hydropathy profile for β-endorphin (peptide 6), the parent peptide of the analogue series used in the present study. While these plots are generally used to determine potential antigenic sites on a polypeptide or protein[18], the data can equally be used to assess the probability that a particular segment of a polypeptide will interact with a particular type of ligand, *e.g.* hydrophobic surfaces. Closer inspection of Fig. 14 reveals that the amino-terminus of β-endorphin can be considered to be polar while the carboxy-terminal segment is largely hydrophobic in nature. As a consequence, analogues which are limited to residues 5–13 should exhibit a lower affinity for hydrocarbonaceous surfaces than analogues derived from the carboxyl-terminus of β-endorphin. Comparison of the log k'_0 values of peptides 10–12 with that of peptide 22 indeed confirms this prediction. A number of previous studies[19–23] have attempted to correlate selectivity properties with summated hydrophobicity ($\Sigma\chi$) values of peptides of different sequences. This approach does not account for the presence of localised hydrophobic segments within a larger peptide of intermediate polarity. As a result, the experimentally observed retentive properties of a series of peptide analogues may not mirror the trend expected on the basis of the corresponding summated hydrophobicity coefficients calculated solely on linear sequence additivity. In this regard, an initial sequence analysis using appropriate hydropathy profiles would thus appear to provide very useful structure–retention information pertinent to the selection of chromatographic conditions.

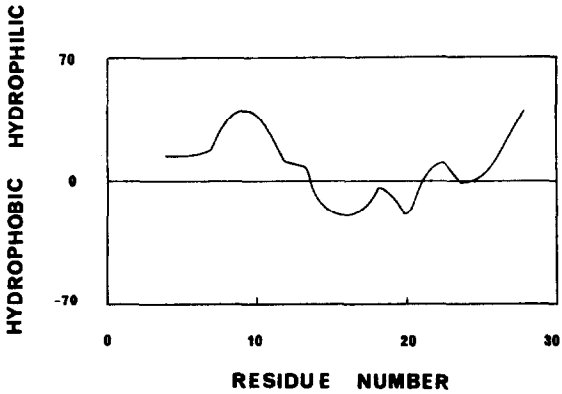

Fig. 14. Hydropathy profile for human β-endorphin (peptide 6, Table II) based on hydrophilicity coefficients. See text for details.

Discrepancies between retention properties and either summated hydrophobicity or linear hydropathy parameters are expected to become more significant as the molecular size of the solute increases. A number of algorithms are available to predict the secondary structure of peptides and proteins, such as the Chou–Fasman[24] method for predicting α-helix and β-sheet formations and other procedures[25,26] which determine the probability of helix formation in a particular solvent environment. These approaches can also be used to assist in locating potential hydrophobic areas on the surface of a molecule via characterisation of amphipathic regions. For example, it is known from circular dichroism studies[27] that the helical content of β-endorphin increases in the presence of anionic lipids. Probability profiles (Fig. 15) indicate than an amphipathic α-helix can form in the carboxy-terminal region of the peptide when it is exposed to a hydrophobic environment. The three-dimensional structure of the helix can be represented by two-dimensional projections of "helical wheels"[28]. Such a wheel is shown in Fig. 16 for the amino- and carboxy-terminal regions of human β-endorphin. The perimeter of the wheel corresponds to the backbone of the peptide chain, and the external spokes represent the individual amino acid side-chains. For an α-helix with 3.6 amino acid residues per turn, adjacent side chains in the sequence are separated by 100° of arc on the wheel. The chromatographic significance of this secondary structure lies in the hydrophobic domain which runs along the length of the right hand side of the helix as represented in Fig. 16b. Therefore, if β-endorphin chromatographed at any time with a carboxy-terminal amphipathic α-helical structure, the segments incorporating (Leu-14)–(Phe-18)–(Ala-21)–(Asn-25) and (Val-15)–(Ile-22)–(Ala-26), would represent the sites most likely to interact with the reversed-phase support. The molecular contact area associated with the first hydrophobic segment can be estimated from known α-helical dimensions to be approximately 136 Å^2. According to solvophobic theory, selectivity for a homologous series of peptide solutes eluted under reversed-phase conditions is

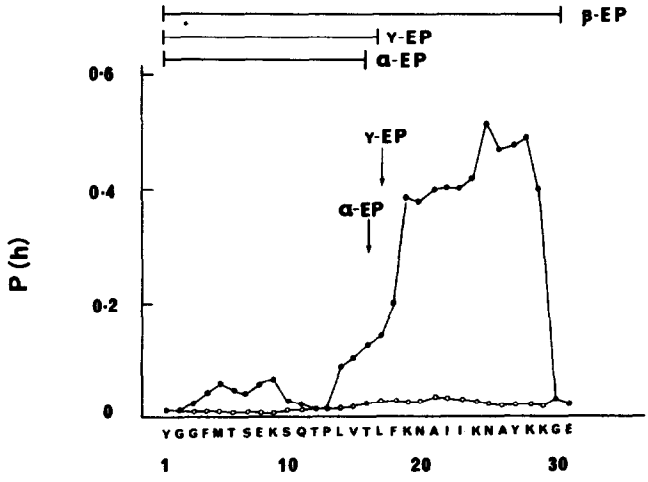

Fig. 15. Helix probability profile for human β-endorphin (peptide 6, Table II) in water (open points) and in the presence of anionic lipids (filled points).

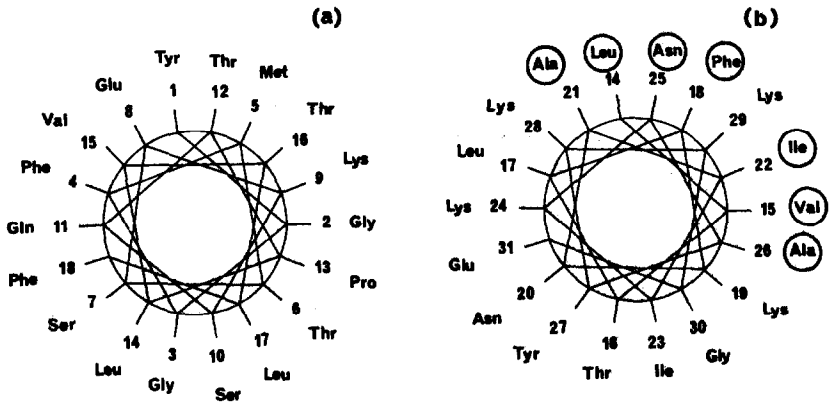

Fig. 16. Representation of the amino-terminal and carboxyl-terminal moieties of human β-endorphin (peptide 6, Table II) on an Edmundson helical wheel[28]. (a) Residues 1–19 (peptide 5, Table II) (b) residues 14–31.

related to mobile phase surface tension by[29]

$$\tau_{i,j} = \log \alpha_{i,j} = \frac{\Delta\,[(\Delta\, G_{vdw})_{i,j} + \gamma N\,(\Delta A_j - \Delta A_i)]}{2.3\,RT} \tag{11}$$

where $\Delta(\Delta G_{vdw})_{i,j}$ is the difference in Van der Waals interaction energies for the solutes i and j, $(\Delta A_j - \Delta A_i)$, equal to $\Delta A_{j,i}$, is the difference in respective molecular contact areas, N is Avogadro's constant, R is the gas constant and T is the absolute temperature. Eqn. 11 predicts a linear relationship between τ and γ with a slope proportional to $\Delta\Delta A$ for a series of solutes. The $\Delta\Delta A$ values for β-endorphin relative to Met^5-enkephalin/peptide 1 were therefore estimated for the four developmental columns using this approach.

Values of $\Delta\Delta A$ equivalent to 62.3, 65.1, 41.9, and 36.3 Å^2 were calculated for the 7.3, 10.0, 13.0 and 30.0 nm pore diameter packing materials respectively. The chromatographic values were therefore lower than the geometrically determined estimates which would represent the maximum theoretical contact area. While the conditions which apply to the use of eqn. 11 may not be directly applicable to heterogenous peptides, chromatographic retention and bandwidth parameters of a series of related peptides will contain a large amount of information regarding the structure of each migrating species. In addition, the presence of a stabilised α-helical structure for β-endorphin gives rise to a number of important considerations regarding the chromatographic performance of this peptide. If for example the affinities of the two hydrophobic segments which could bind independently to the stationary phase were significantly different to the affinities of the interactive sites present in a random coil structure, different rates of adsorption–desorption would occur. While this will not be detectable in S and log k'_0 values (*i.e.* directly from the retention data), these kinetic effects would be manifested as anomalous band-broadening. Furthermore, the presence of a lipid-stabilised α-helical segment will result in a decrease in the molecular size of the β-endorphin peptide. Indeed, it has been observed that β-en-

dorphin undergoes a decrease in molecular volume when chromatographed in size exclusion systems in the presence of acidic lipids[30].

If this conformational reorientation proceeds during the course of the chromatographic separation, then differences in diffusional properties from those expected for a fully random coil structure will result because of the differential migration of the solute. This will again lead to peak widths which are larger than anticipated on the basis of the general plate height theory for rigid small molecular weight substances. A similar helical analysis can be carried out for peptides 5 (Fig. 11a) and 22 which represent the amino- and carboxy-terminal moieties of β-endorphin. While it is unlikely that these peptides will exist as highly stabilised helical structures, it is possible that the peptides may explore a number of other conformational preferences. An α-helical structure may therefore represent a transient species in the reorientation pathway that the solute follows either in the mobile phase or at the stationary phase surface. Since peptide helical structure cannot be monitored in chromatographic systems at the stationary phase surface by conventional techniques such as circular dichroism alternative spectroscopic methods are required, *i.e.* Fourier transform infrared (FTIR) spectral analysis. Recent spectroscopic studies[31] on the conformation of proteins adsorbed onto C_8 alkyl-bonded silica in the presence of increasing concentrations of organic modifier using such solid–liquid state FTIR procedures have clearly demonstrated the existence of surface-associated protein conformational changes induced by organic solvents.

Experimentally, it is reasonably straight forward to chromatographically detect gross conformational changes in peptides and proteins, where two folded forms have significantly different hydrophobic characteristics and thus different retention times. Accurate quantitation of the more subtle effects of small shifts in conformational equilibria which may be induced by interaction with a polar or non-polar surface clearly requires more sophisticated approaches to the analysis of chromatographic data. As a result the precise structural integrity of a chromatographically purified protein sample cannot be assumed solely because of the elution of symmetrical peaks of band-broadening identical to those predicted from plate theory of small organic molecules. The present study highlights further the issue of structure–retention relationships in reversed-phase chromatography as it applies to polypeptides and proteins analysis and purification. The ability to utilise similar experimental methods to detect and characterise conformational reorientation processes with HPLC systems thus represents a powerful tool to investigate general physico-chemical phenomena associated with the interaction of proteins with chemically modified surfaces or other macromolecules.

ACKNOWLEDGEMENTS

This investigation was supported by grants from the National Health and Medical Research Council of Australia to M. T. W. Hearn.

REFERENCES

1 L. R. Snyder, in Cs. Horváth, (Editor), *High Performance Liquid Chromatography*, Vol. 1, Academic Press, New York, NY, 1980, p. 208.
2 M. I. Aguilar, A. N. Hodder and M. T. W. Hearn, *J. Chromatogr.*, 327 (1985) 115.

3 M. T. W. Hearn, in J. Navratil (Editor), *Separation Science and Technology*, Vol. 1, Litarvan Press, Colorado, 1986, pp. 270–293.
4 M. A. Stadalius, H. S. Gold and L. R. Snyder, *J. Chromatogr.*, 296 (1984) 31.
5 M. T. W. Hearn and M. I. Aguilar, *J. Chromatogr.*, 359 (1986) 31.
6 M. Kunitani, P. Hirtzer, D. Johnson, R. Halenbeck, A. Boosman and K. Koths, *J. Chromatogr.*, 359 (1986) 391.
7 M. T. W. Hearn and B. Grego, *J. Chromatogr.*, 282 (1983) 541.
8 M. T. W. Hearn and M. I. Aguilar, *J. Chromatogr.*, 352 (1986) 35.
9 M. T. W. Hearn, A. N. Hodder and M. I. Aguilar, *J. Chromatogr.*, 327 (1985) 47.
10 X. Geng and F. E. Regnier, *J. Chromatogr.*, 296 (1984) 15.
11 M. T. W. Hearn and M. I. Aguilar, *J. Chromatogr.*, 392 (1987) 33.
12 M. T. W. Hearn and B. Grego, *J. Chromatogr.*, 266 (1983) 75.
13 K., K. Unger, G. Jilge, J. N. Kinkel and M. T. W. Hearn, *J. Chromatogr.*, 359 (1986) 61.
14 M. T. W. Hearn and K. K. Unger, *J. Chromatogr.*, submitted.
15 X. M. Lu, K. Benedek and B. L. Karger, *J. Chromatogr.*, 359 (1986) 19.
16 J. Jacobson, W. Melander, G. Vaisnys and C. Horvath, *J. Phys. Chem.*, 88 (1984) 4356.
17 M. T. W. Hearn, in J.-C. Janson (Editor), *High Resolution Protein Purification*, Verlag Chemie, Deerfield Beach, 1987, in press.
18 J. M. R. Parker, D. Guo and R. S. Hodges, *Biochemistry*, 25 (1986) 5425.
19 R. F. Rekker and H. M. de Kart, *Eur. J. Med. Chem.*, 14 (1979) 479.
20 C. A. Browne, H. P. J. Bennett and S. Solomon, *Anal. Biochem.*, 124 (1982) 201.
21 S. J. Su, B. Grego, B. Niven and M. T. W. Hearn, *J. Liq. Chromatogr.*, 4 (1981) 1945.
22 J. L. Meek and Z. L. Rossetti, *J. Chromatogr.*, 211 (1981) 15.
23 D. Guo, C. T. Mant, A. K. Taneja, J. M. R. Parker and R. S. Hodges, *J. Chromatogr.*, 359 (1986) 499.
24 P. Y. Chou and G. D. Fasman, *Biochemistry*, 13 (1974) 222.
25 W. L. Mattice and R. M. Robinson, *Biochem. Biophys. Res. Com.*, 101 (1981) 1311.
26 M. H. Hecht, B. O. Zweifel, H. A. Scheraga, *Macromolecules*, 11 (1978) 545.
27 J. T. Yang, T. A. Bewley, G. C. Chen and C. H. Li, *Proc. Natl. Acad. Sci. U.S.A.*, 74 (1977) 3235.
28 M. Schiffer and A. B. Edmundson, *Biophys. J.*, 7 (1967) 121.
29 Cs. Horváth, W. Melander and I. Molnar, *J. Chromatogr.*, 125 (1976) 129.
30 J. E. Bolton, J. H. Livesey and M. T. W. Hearn, *J. Liq. Chromatogr.*, 7 (1984) 1089.
31 G. E. Katzenstein, S. A. Vrona, R. J. Wechsler, B. L. Steadman, R. V. Lewis and C. R. Middaugh, *Proc. Natl. Acad. Sci. U.S.A.*, 83 (1986) 4268.